Tumor Necrosis Factor-α Promotes Phosphoinositide 3-Kinase Enhancer A and AMP-Activated Protein Kinase Interaction to Suppress Lipid Oxidation in Skeletal Muscle

Margaret Chui Ling Tse,[1] Oana Herlea-Pana,[2] Daniel Brobst,[2] Xiuying Yang,[2,3] John Wood,[2] Xiang Hu,[2] Zhixue Liu,[2] Chi Wai Lee,[1] Aung Moe Zaw,[4] Billy K.C. Chow,[4] Keqiang Ye,[5] and Chi Bun Chan[4]

Diabetes 2017;66:1858–1870 | https://doi.org/10.2337/db16-0270

Tumor necrosis factor-α (TNF-α) is an inflammatory cytokine that plays a central role in obesity-induced insulin resistance. It also controls cellular lipid metabolism, but the underlining mechanism is poorly understood. We report in this study that phosphoinositide 3-kinase enhancer A (PIKE-A) is a novel effector of TNF-α to facilitate its metabolic modulation in the skeletal muscle. Depletion of PIKE-A in C2C12 myotubes diminished the inhibitory activities of TNF-α on mitochondrial respiration and lipid oxidation, whereas PIKE-A overexpression exacerbated these cellular responses. We also found that TNF-α promoted the interaction between PIKE-A and AMP-activated protein kinase (AMPK) to suppress its kinase activity in vitro and in vivo. As a result, animals with *PIKE* ablation in the skeletal muscle per se display an upregulation of AMPK phosphorylation and a higher preference to use lipid as the energy production substrate under high-fat diet feeding, which mitigates the development of diet-induced hyperlipidemia, ectopic lipid accumulation, and muscle insulin resistance. Hence, our data reveal PIKE-A as a new signaling factor that is important for TNF-α–initiated metabolic changes in skeletal muscle.

Tumor necrosis factor-α (TNF-α) is a cytokine that plays significant roles in multiple cellular processes. Initially discovered as an anticancer agent, TNF-α is now recognized as an important contributor to autoimmune diseases, neurological disorders, cardiovascular disorders, pulmonary diseases, and metabolic syndromes (1). In obese subjects, the amount of circulating TNF-α is drastically increased, which is a result of enhanced expression in the adipose tissues and the infiltrated macrophages (2,3). Numerous studies have demonstrated a causal linkage of high TNF-α level and tissue insulin resistance. TNF-α activates c-Jun N-terminal kinase (JNK) to phosphorylate and suppress the activity of insulin receptor (IR) substrate 1 (4). Consequently, the insulin-induced signaling is disrupted, leading to impaired glucose uptake in multiple tissues (5,6). TNF-α also provokes activation of the transcription factor nuclear factor- κB, which causes the expression of genes like tyrosine phosphatase-1B and suppression of cytokine signaling proteins to antagonize the insulin signaling (7,8). In addition to modifying the glucose metabolism, TNF-α is involved in lipid use. For instance, infusion of TNF-α in human enhances whole-body lipolysis (9). Several studies have also shown that TNF-α enhances lipid accumulation in the liver by regulating the activities of lipoprotein lipase, hormone-sensitive lipase, and adipocyte triglyceride (TG) lipase (10,11). In cultured myotubes, TNF-α suppresses the activities of AMP-activated protein kinase (AMPK), reduces fatty acid (FA) oxidation, and enhances lipid accumulation (12).

AMPK is a serine-threonine kinase that consists of α, β, and γ subunits. It is the key sensor that coordinates various metabolic processes to meet the cellular energy demand in response to different stresses. AMPK can be activated by

[1]School of Biomedical Sciences, The University of Hong Kong, Hong Kong SAR, People's Republic of China
[2]Department of Physiology, University of Oklahoma Health Sciences Center, Oklahoma City, OK
[3]Drug Screening Center, Institute of Materia Medica, Beijing, People's Republic of China
[4]School of Biological Sciences, The University of Hong Kong, Hong Kong SAR, People's Republic of China
[5]Department of Pathology and Laboratory Medicine, Emory University School of Medicine, Atlanta, GA

Corresponding author: Chi Bun Chan, chancb@hku.hk.

Received 26 February 2016 and accepted 29 March 2017.

This article contains Supplementary Data online at http://diabetes.diabetesjournals.org/lookup/suppl/doi:10.2337/db16-0270/-/DC1.

© 2017 by the American Diabetes Association. Readers may use this article as long as the work is properly cited, the use is educational and not for profit, and the work is not altered. More information is available at http://www.diabetesjournals.org/content/license.

Downloaded from http://diabetes.diabetesjournals.org/diabetes/article-pdf/66/7/1858/539888/db160270.pdf by guest on 24 April 2024

AMP binding or phosphorylation by other kinases like liver kinase B1 or Ca^{2+}/calmodulin-dependent protein kinase kinase β (13,14). When energy supply is insufficient (e.g., fasting and exercise), cellular AMPK is activated and phosphorylates the downstream acetyl-CoA carboxylase (ACC), which promotes the mitochondrial transportation of FA for β-oxidation and hence elevated ATP production (15). Interestingly, AMPK activity is reduced in obese animals, which is likely a result of dysregulated lipid metabolism and insulin resistance (16–18). The molecular mechanism that impairs AMPK activity in obese tissues remains largely unknown, although Steinberg et al. (12) suggest that TNF-α may induce phosphatase 2C (PP2C) expression to dephosphorylate AMPK.

Phosphoinositide 3-kinase enhancer A (PIKE-A) is a ubiquitously expressed GTPase that belongs to the Centaurin family (19). As a proto-oncogene with high expression in a variety of cancers (20), our studies showed that PIKE-A interacted with Akt directly to potentiate its kinase activity (21). Given that Akt is the downstream effector of insulin to promote glucose uptake (22), the interaction between PIKE-A and Akt may represent a regulatory node for glucose metabolism. Indeed, liver-specific depletion of *PIKE* results in hepatic insulin resistance and the development of diabetes phenotypes (22). This metabolic defect is mainly caused by incomplete IR activation, as PIKE-A is an IR kinase enhancer for insulin to fully activate IR (22). Although the whole-body *PIKE* knockout ($PIKE^{-/-}$) mice display a hepatic insulin resistance, surprisingly, these animals have higher systemic insulin sensitivities and are resistant to diet-induced obesity, which is possibly an outcome of enhanced AMPK activity in white adipose tissue (WAT) and skeletal muscle (23). Nevertheless, it remains unclear why depletion of *PIKE* leads to AMPK upregulation. In this report, we demonstrate that PIKE-A is a downstream effector of TNF-α to control the cellular metabolism through interacting and modulating the activity of AMPK.

RESEARCH DESIGN AND METHODS

Generation of Muscle-Specific PIKE Knockout Mice

Muscle-specific PIKE knockout (MPKO) mice were generated by crossing *PIKE Flox/Flox* mice (24) with transgenic mice that carry the muscle creatine kinase promoter-driven Cre (mCK-Cre; The Jackson Laboratory). Genotyping was performed by PCR using genomic DNA extracted from the tail (22). Total RNA was extracted from mouse tissues using TRIzol Reagent (Invitrogen). The primers used in RT-PCR were 5′−ACAGGATCAGTGCATCATCTC-3′ (PIKE forward), 5′-CTGCCCAGCTACAGGAGTAG-3′ (PIKE reverse), 5′-CG CATCTTCTTGTGCAGTGCC-3′ (GAPDH forward), and 5′-GGCCTTGACTGTGCCGTTGAATTT-3′ (GAPDH reverse). All in vivo assays were done in 8-week-old female mice because of the sex-dimorphic effect in *PIKE*-null animals (23) and were approved by the Institutional Animal Care and Use Committee of the University of Oklahoma Health Sciences Center.

Cell Culture

C2C12 myoblasts were cultured in DMEM with 5% FBS, 15% calf serum, 100 IU/mL penicillin, and 100 μg/mL streptomycin (Invitrogen). Differentiation of myoblasts into myotubes was performed by incubating 100% confluent myoblast with differentiating medium (2% horse serum, 100 IU/mL penicillin, and 100 μg/mL streptomycin) for 4 days. Differentiation of the C2C12 was confirmed by morphological changes as reported (25).

Western Blot and Immunoprecipitation

Tissue extracts were prepared by homogenizing the tissues in lysis buffer (50 mmol/L Tris [pH 7.4], 40 mmol/L NaCl, 1 mmol/L EDTA, 0.5% Triton X-100, 1.5 mmol/L Na_3VO_4, 50 mmol/L NaF, 10 mmol/L $Na_4P_2O_7$, 10 mmol/L sodium β-glycerol phosphate, and protease inhibitor cocktail). Cell debris was removed by centrifugation, and the supernatants were collected for further analysis. Anti-PIKE and antitubulin antibodies were obtained from Bethyl Laboratories and Santa Cruz Biotechnology, respectively. All other antibodies were purchased from Cell Signaling Technology.

AMPK Kinase Assay

AMPK in C2C12 myotubes was immunoprecipitated using anti-AMPKα antibody (Cell Signaling Technology). After washing extensively with lysis buffer, the kinase activity against IR substrate 1 peptide was determined using the Cyclex AMPK Kinase Assay Kit (MBL International) as reported (26,27).

Determination of Mitochondrial Content

Total DNA was isolated by DNAeasy kit (Qiagen). The amount of mitochondrial DNA was determined by real-time PCR using the primers 5′-CCCAGCTACTACCATCATTCAA GT-3′ (forward) and 5′-GATGGGTTTGGGAGATTGGTTGA TGT-3′ (reverse) as reported (28). The amount of β-actin gene in the genomic DNA was also examined (to normalize any variation because of the difference of total DNA extracted).

Adenovirus

Adenoviruses that overexpress PIKE-A or short hairpin RNA against PIKE (shPIKE) (24) were prepared and purified using the Adeno-X Maxi Purification Kit (Clontech Laboratories). Virus infection was performed by adding 1×10^5 or 5×10^5 plaque-forming units/well to 96- or 6-well plates, respectively, for 24 h to induce overexpression or gene silencing.

Determination of Mitochondrial Respiration and Lipid Oxidation

Mitochondrial respiration of C2C12 myotubes was determined by the XFe 96 Extracellular Flux Analyzer using the XF Mito Stress Test Kit (Seahorse Bioscience). The concentrations of oligomycin, carbonyl cyanide-*p*-trifluoromethoxyphenylhydrazone, antimycin A, and rotenone used were 100, 100, 100, and 50 μm, respectively. The oxygen

Downloaded from http://diabetes.diabetesjournals.org/diabetes/article-pdf/66/7/1858/539888/db160270.pdf by guest on 24 April 2024

consumption rate (OCR) and extracellular acidification rate were recorded, and the respiration rates were calculated as instructed by the manufacturer. OCR from exogenous lipid oxidation of C2C12 myotubes was determined by Extracellular Flux Analyzer using the XF Palmitate-BSA FAO Substrate (Seahorse Bioscience) as reported (29). One mmol BSA-coupled palmitic acid (PA) and 40 μmol/L etomoxir were used in the analysis.

TNF-α Infusion and Infliximab Treatment

In vivo TNF-α (1 μg/kg/day) infusion was performed by implanting the Osmotic pump (Model 1003D; Alzet) containing recombinant human TNF-α (Invitrogen) into the interscapular region of female C57BL/6 mice as reported previously (12). Twenty-four hours after implantation, the animals were euthanized to collect the tissues for various biochemical analyses.

Female C57BL/6 mice (5- to 6-month-old) that were fed with a high-fat diet (HFD) for 12 weeks were i.p. injected with infliximab (50 μg/mouse/day) as reported (30). After 8 days of treatment, serum and hind limb skeletal muscles (mixed fiber type) were collected and used for biochemical analysis.

Analytical Procedures

Eight-week-old female mice were fed with chow or HFD (60% kcal; Research Diets Inc.) for 14 weeks. Fasting was performed by removing the food from the home cage for 16 h. Blood glucose level was measured by Accu-Chek Advantage Blood Glucose Meter (F. Hoffmann-La Roche Ltd.). Serum insulin, leptin (Crystal Chem), and TNF-α (R&D Systems) were measured by ELISA. Serum and tissue lipid levels were determined by the Triglyceride Quantification Kit, Free Fatty Acid Quantification Kit, or Total Cholesterol and Cholesteryl Ester Colorimetric Assay Kit (BioVision). Glucose tolerance test was performed on overnight-fasted (16 h) mice after peritoneal injection of D-glucose (2 g/kg of body weight). Hematoxylin and eosin staining was performed on paraffin-embedded sections using standard procedures. Adipocyte size was measured by the software ImageJ (National Institutes of Health).

In Vivo Insulin Stimulation

Saline or 5 U human insulin (Eli Lilly and Company) was injected into the inferior vena cava of the overnight-fasted (16 h) mice. After 5 min, liver and hind limb muscles (mixed fiber types) were removed and immediately frozen in liquid nitrogen.

Hyperinsulinemic-Euglycemic Clamp, Metabolic Cage, Body Composition Determination, and Locomotion Analysis

Systemic glucose metabolisms including glucose infusion rate, glucose turnover rate, and glucose uptake and hepatic glucose output were determined by hyperinsulinemic-euglycemic clamp (insulin: 2.5 mU/kg/min) as previously reported (23). Fat and lean masses of the animals were determined by H1-MRS (EchoMRI). Computerized metabolic cages (Labmaster cages, TSE Systems; and Comprehensive Lab Animal Monitoring System, Columbus Instruments) were used in awake mice to simultaneously measure oxygen consumption, CO_2 production, energy expenditure, indirect calorimetry, and food/water intake over 3 days. The metabolic parameters were all normalized to the lean mass of the animals. Physical activity of the mouse was detected using the locomotion recording chamber (transparent Plexiglas cages placed into a rack with seven infrared photobeams spaced 5 cm apart (San Diego Instruments) as previously reported (23).

Statistical Analysis

Results were expressed as mean ± SEM and considered significant when P was <0.05. Statistical analysis was performed using Student t test, one-way ANOVA, or two-way ANOVA followed by a Tukey multiple-comparison test or Bonferroni posttest by computer program (Prism; GraphPad Software).

RESULTS

MPKO Mice Are Obesity Resistant

Global deletion of *PIKE* in mice protects the animals from diet-induced obesity through AMPK upregulation (23). However, these $PIKE^{-/-}$ animals also display enhanced physical activity (23,31). Because exercise is an activator of AMPK (32), it is reasonable to suspect that the augmented AMPK activity in $PIKE^{-/-}$ muscle is a result of increased locomotion but not a cell-autonomous effect. To address this issue and specifically study the functions of PIKE-A in skeletal muscle, we generated the MPKO mice by Cre/Lox recombination (Supplementary Fig. 1*A*). Because only female $PIKE^{-/-}$ mice showed lean phenotypes (23), we thus used female animals in our analyses. Tissue-specific ablation of *PIKE* was confirmed by genomic PCR, RT-PCR, and immunoblotting (Supplementary Fig. 1*B–D*). Body weights of MPKO and *Fl/Fl* mice were similar under chow diet feeding (Supplementary Fig. 2*A*). Circulating leptin, TNF-α, and lipid contents (Supplementary Fig. 2*B–D*) were also comparable between genotypes. The hepatic TG and free FA (FFA) acid content were not significantly altered (Supplementary Fig. 2*E*), but muscular TG was reduced in MPKO mice (Supplementary Fig. 2*F*). When the animals were fed with an HFD, a significant reduction of body weight gain was recorded in MPKO mice (Fig. 1*A*). These animals exhibited a reduction of total fat mass (Fig. 1*B*) and adipocyte size (Fig. 1*C* and *D*). Total lean mass was comparable between the two genotypes after HFD feeding (Fig. 1*B*). The concentrations of circulating leptin (Fig. 1*E*), TNF-α (Fig. 1*F*), cholesterol, TG, and FFA (Fig. 1*G*) were significantly lower in HFD-fed MPKO mice. Moreover, hepatic concentrations of TG and FFA (Fig. 1*H*) were diminished in MPKO animals, which fit with the reduced hepatic steatosis observed in the histological analysis (Fig. 1*C*). TG and FFA concentrations in the skeletal muscle were also decreased in the HFD-fed MPKO mice (Fig. 1*I*). In contrast,

Downloaded from http://diabetes.diabetesjournals.org/diabetes/article-pdf/66/7/1858/539888/db160270.pdf by guest on 24 April 2024

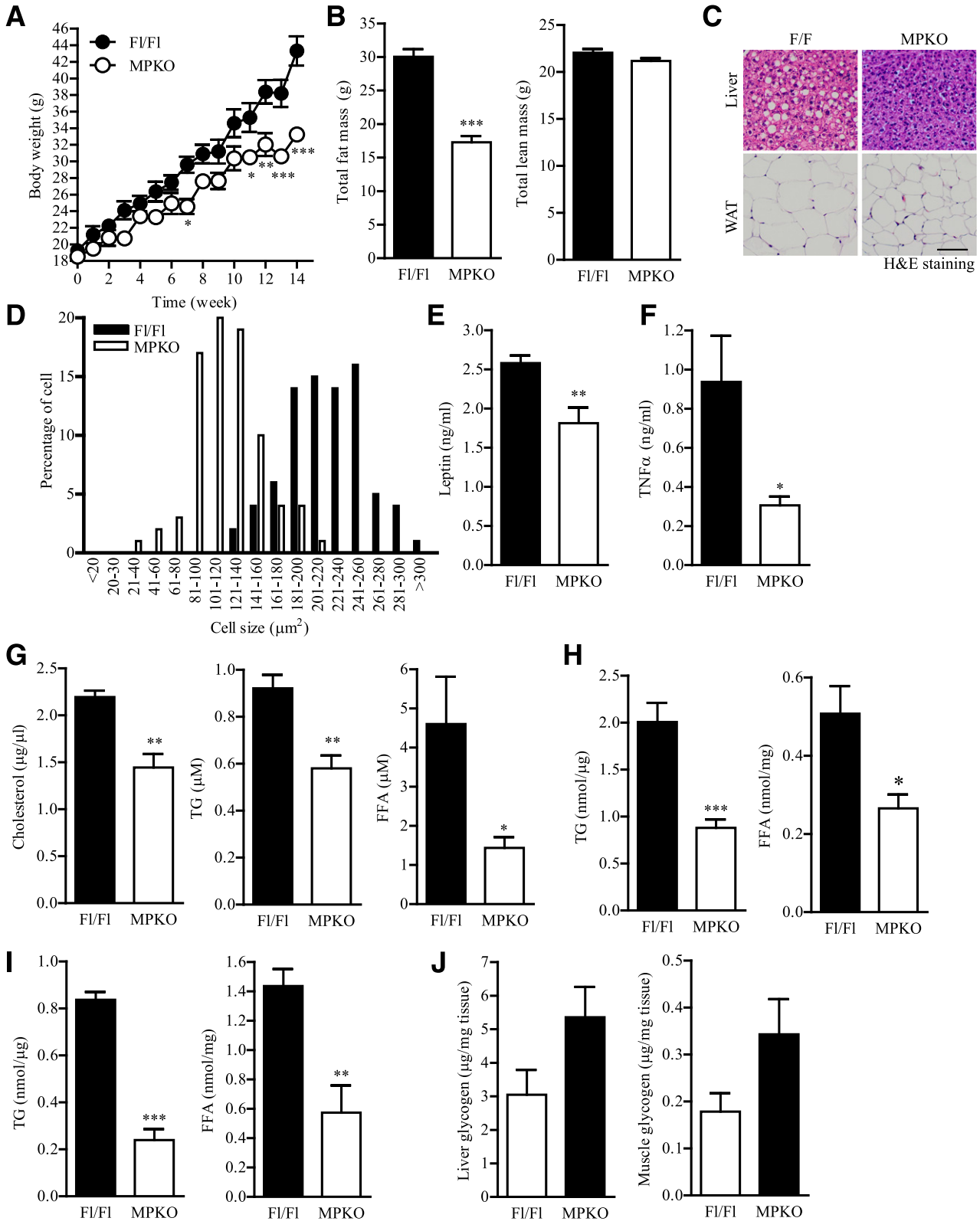

Figure 1—MPKO mice are obesity resistant. *A*: Growth curve of 8-week-old mice fed with HFD (60% kcal; **P* < 0.05; ***P* < 0.01; ****P* < 0.001, two-way ANOVA; *n* = 6). *B*: Body composition of mice that have been fed with HFD for 14 weeks (****P* < 0.001, Student *t* test; *n* = 5 to 6). *C*: Representative pictures of hematoxylin and eosin (H&E) staining of liver and inguinal WAT and sections from mice that have been fed with HFD for 14 weeks. Scale bar, 50 μm. *D*: Adipocyte size distribution of inguinal WAT from mice that have been fed with HFD for 14 weeks (*n* = 6). *E*: Circulating leptin concentration in mice that have been fed with HFD for 14 weeks (***P* < 0.01, Student *t* test; *n* = 6). *F*: Circulating TNF-α concentration in mice that have been fed with HFD for 14 weeks (**P* < 0.05, Student *t* test; *n* = 6). *G*: Circulating lipid contents in mice that have been fed with HFD for 14 weeks (**P* < 0.05; ***P* < 0.01, Student *t* test; *n* = 6). *H*: Hepatic lipid contents in mice that have been fed with HFD

Downloaded from http://diabetes.diabetesjournals.org/diabetes/article-pdf/66/7/1858/539888/db160270.pdf by guest on 24 April 2024

the amount of hepatic and muscular glycogen was slightly higher in MPKO muscle (Fig. 1*J*). These data suggest that muscular PIKE-A is involved in body weight control and lipid metabolism under a normal feeding regimen, but depletion of *PIKE* in the skeletal muscle alleviates the diet-induced body weight gain, hyperlipidemia, and ectopic lipid accumulation.

Ablation of *PIKE* in the Muscle Shifts the Substrate Usage for Energy Production

We next determined how *PIKE* ablation in muscle alleviates obesity development. MPKO animals displayed no locomotion abnormalities in the beam-break assay (Fig. 2*A*). Daily food intake, but not the water uptake, was significantly reduced in HFD-fed MPKO mice (Fig. 2*B* and *C*). Total oxygen consumption was similar between the two genotypes after HFD feeding (Fig. 2*D*). However, a significant decrease of CO_2 production was recorded in HFD-fed MPKO mice (Fig. 2*E*), which caused a lower respiratory exchange ratio than the *Fl/Fl* control (Fig. 2*F*). Ablation of *PIKE* in muscle did not change the overall energy expenditure of the animals (Fig. 2*G*), indicating muscular PIKE-A is only important in controlling substrate use for energy production but not modulating the overall energy expenditure. Because AMPK is a central regulator of lipid oxidation, we tested if AMPK activity was upregulated in the MPKO muscle. Although we did not observe any significant changes in AMPK phosphorylation in the tissues of chow-fed MPKO mice (Supplementary Fig. 3), muscular AMPKα T172 and ACC S79 phosphorylations were increased in the HFD-fed MPKO mice (Fig. 2*H*). AMPK and ACC phosphorylation in the WAT were also elevated, which is possibly an outcome of reduced body weight (Fig. 2*H*). In contrast, AMPK phosphorylation was comparable between MPKO and *Fl/Fl* livers (Fig. 2*H*). It is interesting to note that both ACC expression and phosphorylation were reduced in MPKO liver (Fig. 2*H*) but the hepatic ratios of phosphorylated ACC to total ACC were comparable between MPKO and *Fl/Fl* mice (Fig. 2*I*). Because AMPK controls lipid oxidation by phosphorylating ACC to enhance mitochondrial FA uptake (15), the elevated AMPK in HFD-fed muscle and WAT provides a possible explanation for the higher lipid usage preference in MPKO mice.

MPKO Mice Are Protected From Diet-Induced Insulin Resistance

Activation of AMPK pharmacologically or genetically improves the insulin sensitivity and glucose handling in a variety of animal models (33,34). Because we observed an upregulation of AMPK in the skeletal muscle of HFD-fed MPKO mice, we thus tested if the MPKO mice have better insulin sensitivity. As expected, the diet-induced hyperglycemia and hyperinsulinemia were alleviated in MPKO mice (Fig. 3*A* and *B*), which are indicators of improved insulin responsiveness in these animals. Indeed, MPKO displayed better performance in the glucose tolerance test (Fig. 3*C*). Concurring with these results, MPKO mice have higher glucose infusion (Fig. 3*D*) and turnover rate (Fig. 3*E*) during the hyperinsulinemic-euglycemic clamp, suggesting insulin induces more glucose uptake in MPKO mice than the *Fl/Fl* animals. In contrast, insulin-suppressed hepatic glucose output was comparable between the two genotypes (Fig. 3*F*). Fitting with these data, insulin injection induced a higher Akt phosphorylation in the skeletal muscle but not the liver of HFD-fed MPKO mice (Fig. 3*G*). Together, our data demonstrate that ablation of *PIKE* in the muscle mitigates diet-induced diabetes in mice.

TNF-α Promotes PIKE-A/AMPK Interaction

To study the regulatory role of PIKE-A on AMPK activity, we first determined if PIKE-A interacts with AMPK directly in the skeletal muscle. Using coimmunoprecipitation, we found that endogenous PIKE-A associated with AMPKα only in the HFD-fed muscle (Fig. 4*A*), implying that PIKE-A/AMPK association is provoked by an unknown metabolic factor during obesity development. AMPK phosphorylation was reduced in the obese muscle (Fig. 4*A*). Given that TNF-α is an AMPK inhibitor (12) and its concentration in the blood is drastically increased in diet-induced obese mice (35), we hypothesized that TNF-α is able to induce PIKE-A/AMPK interaction, which causes a reduction of AMPK activity. To test this hypothesis, we monitored the PIKE-A/AMPK association in the TNF-α–administrated muscle. In vivo infusion of TNF-α to mouse induced a robust JNK p46 phosphorylation and provoked PIKE-A/AMPK association in the skeletal muscle (Fig. 4*B*). In parallel to the formation of PIKE-A/AMPK complex, AMPK and ACC activity were reduced (Fig. 4*B*), which confirmed the previous report that TNF-α is an inhibitory cytokine to these enzymes (12).

To demonstrate that the formation of PIKE-A/AMPK complex is a direct consequence of TNF-α stimulation to the skeletal muscle, we examined if TNF-α triggered PIKE-A/AMPK association in cultured muscle cells. In differentiated C2C12 myotubes, TNF-α challenge increased JNK phosphorylation but reduced AMPK and ACC

for 14 weeks (*$P < 0.05$; ***$P < 0.001$, Student *t* test; $n = 6$). *I*: Lipid content in the hind limb skeletal muscle (mixed fiber type) of mice that have been fed with HFD for 14 weeks (**$P < 0.01$; ***$P < 0.001$, Student *t* test; $n = 6$). *J*: Glycogen content in the liver and hind limb skeletal muscle (mixed fiber type) of mice that have been fed with HFD for 14 weeks ($n = 4$ to 5).

Downloaded from http://diabetes.diabetesjournals.org/diabetes/article-pdf/66/7/1858/539888/db160270.pdf by guest on 24 April 2024

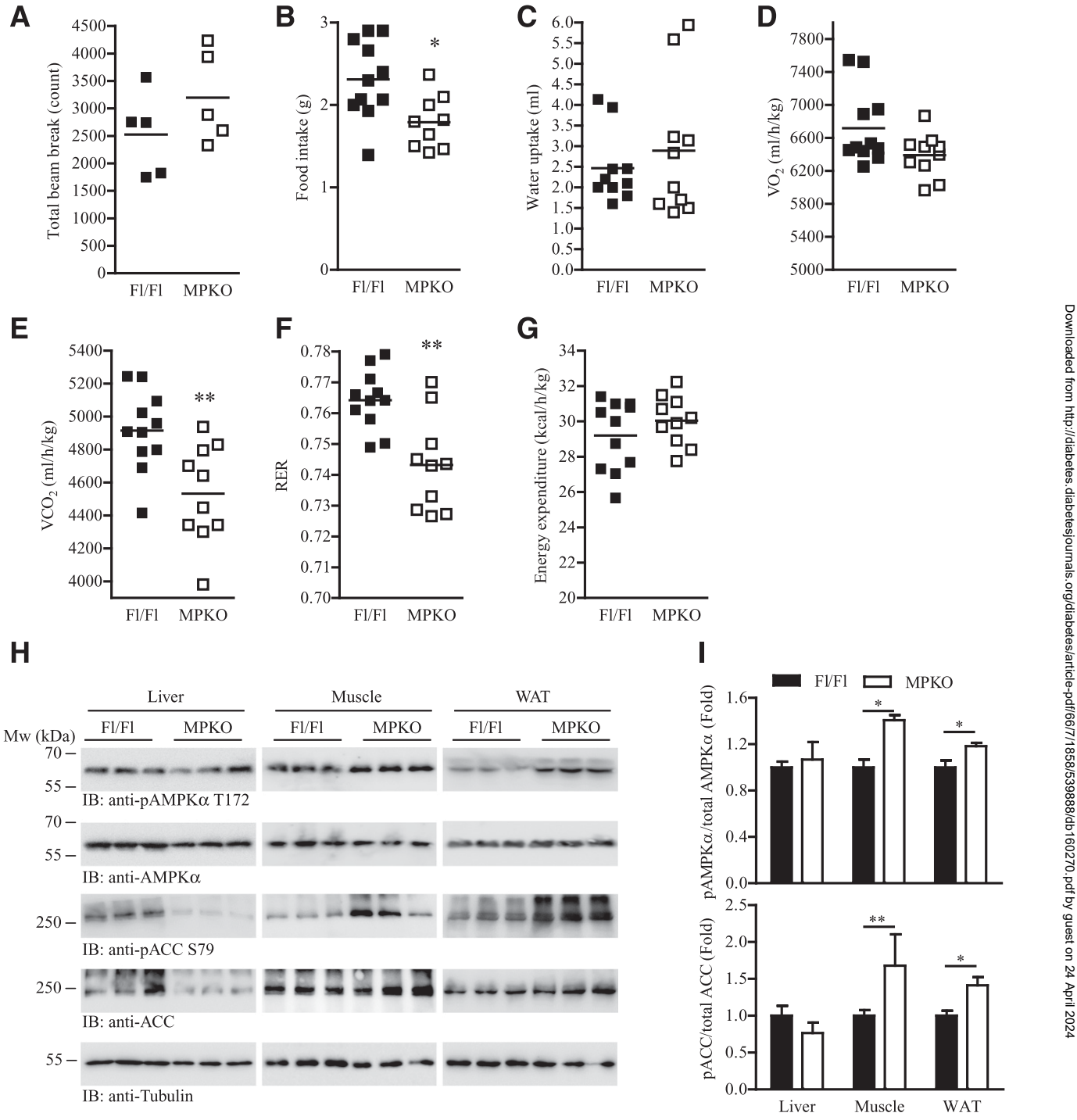

Figure 2—Depletion of PIKE-A in the skeletal muscle shifts the energy substrate usage preference. *A*: Locomotor activity of chow-fed mice as determined by beam-break assay. *B*: Food intake of mice that have been fed with HFD for 14 weeks during the metabolic cage measurement (*$P < 0.05$, Student *t* test). *C*: Water uptake of mice that have been fed with HFD for 14 weeks during the metabolic cage measurement. *D*: Oxygen consumption of mice that have been fed with HFD for 14 weeks during the metabolic cage measurement. *E*: Carbon dioxide production from mice that have been fed with HFD for 14 weeks during the metabolic cage measurement (**$P < 0.01$, Student *t* test). *F*: Respiratory exchange ratio (RER) of mice that have been fed with HFD for 14 weeks during the metabolic cage measurement (**$P < 0.01$, Student *t* test). *G*: Energy expenditure of mice that have been fed with HFD for 14 weeks during the metabolic cage measurement. *H*: Immunoblot (IB) analysis of liver, inguinal WAT, and hind limb muscle (mixed fiber type) isolated from mice that have been fed with HFD for 14 weeks. *I*: Quantification of the immunoblots shown in *H* (*$P < 0.05$; **$P < 0.01$, Student *t* test; $n = 3$). pACC, phosphorylated ACC; pAMPKα, phosphorylated AMPKα.

Downloaded from http://diabetes.diabetesjournals.org/diabetes/article-pdf/66/7/1858/539888/db160270.pdf by guest on 24 April 2024

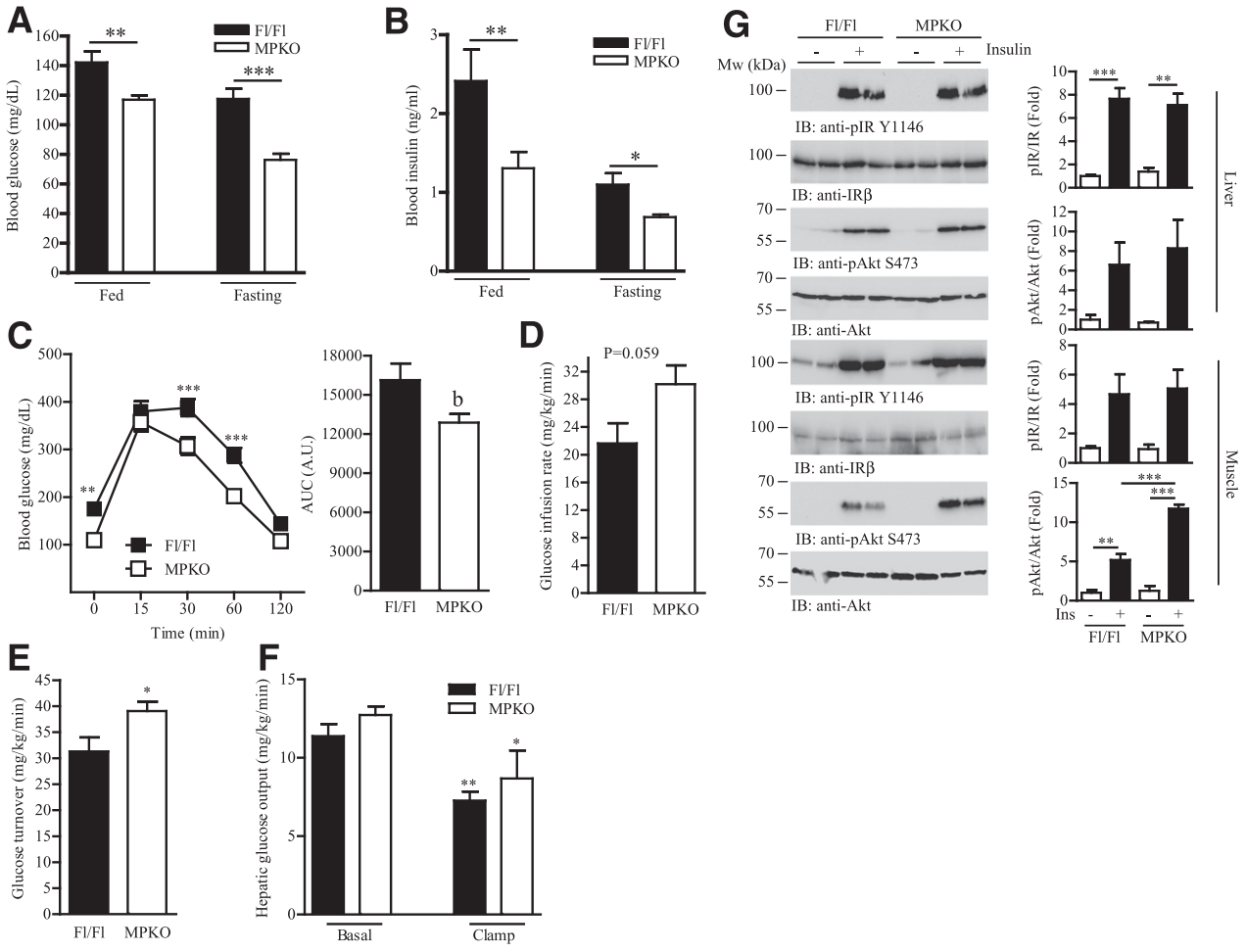

Figure 3—Ablation of *PIKE* gene in the skeletal muscle alleviates diet-induced insulin resistance. *A*: Blood glucose concentration in mice that have been fed with HFD for 14 weeks (**$P < 0.01$; ***$P < 0.001$, Student *t* test; $n = 6$). *B*: Circulating insulin concentration in mice that have been fed with HFD for 14 weeks (*$P < 0.05$; **$P < 0.01$, Student *t* test; $n = 6$). *C*: Glucose tolerance test in mice that have been fed with HFD for 14 weeks (**$P < 0.01$; ***$P < 0.001$, two-way ANOVA; $^{b}P < 0.01$, Student *t* test; $n = 12$). *D*: Glucose infusion rate in mice that have been fed with HFD for 14 weeks during the hyperinsulinemic-euglycemic clamp experiment ($n = 6$, Student *t* test). *E*: Glucose turnover rate in mice that have been fed with HFD for 14 weeks during the hyperinsulinemic-euglycemic clamp experiment (*$P < 0.05$, Student *t* test; $n = 6$). *F*: Hepatic glucose production in mice that have been fed with HFD for 14 weeks during the hyperinsulinemic-euglycemic clamp experiment (*$P < 0.05$; **$P < 0.01$, one-way ANOVA vs. the same genotype; $n = 6$). *G*: Representative result of immunoblotting (IB) analysis in hind limb skeletal muscle (mixed fiber type) and liver of female mice that have been fed with HFD for 14 weeks. Quantification of the immunoblotting analysis is also shown in right panel (**$P < 0.01$; ***$P < 0.001$, one-way ANOVA; $n = 3$). A.U., arbitrary units; AUC, area under the curve; pAkt, phosphorylated Akt; pIR, phosphorylated insulin receptor.

phosphorylations (Fig. 4*C*). In parallel with the downregulation of AMPK activity, TNF-α promoted PIKE-A/AMPK interaction in a time-dependent manner (Fig. 4*C*). We also found that the TNF-α dose-dependently induced PIKE-A/AMPK complex formation in C2C12 myotubes (Fig. 4*D*).

To further prove that high circulating TNF-α is the major contributor to PIKE-A/AMPK interaction in obese muscle, we tested if neutralizing TNF-α in diet-induced obese mice would abolish the formation of PIKE-A/AMPK complex. As shown in Fig. 4*E*, HFD-fed mice treated with TNF-α–neutralizing antibody infliximab (36) displayed a significant reduction of circulating TNF-α. AMPK phosphorylation in infliximab-treated skeletal muscle was increased, whereas the interaction between PIKE-A/AMPK was reduced (Fig. 4*F*). Together, our data demonstrate that TNF-α is the stimulatory factor that controls PIKE-A and AMPK interaction in muscle.

PIKE-A Is Important for TNF-α to Inhibit AMPK Activity and Lipid Oxidation

To verify if PIKE-A is involved in TNF-α–provoked AMPK inactivation and lipid oxidation impairment, we manipulated the amount of PIKE-A in C2C12 cells by infecting the myotubes with an adenovirus that overexpresses PIKE-A (Ad-PIKE-A) or shPIKE (Ad-shPIKE) (22,24). Although TNF-α stimulation reduces the kinase activity of AMPK to ∼62% of the control cells, Ad-PIKE-A infection further potentiates the inhibition to 53% (Fig. 5*A*). The presence of TNF-α also resulted in a decrease of cellular

Downloaded from http://diabetes.diabetesjournals.org/diabetes/article-pdf/66/7/1858/539888/db160270.pdf by guest on 24 April 2024

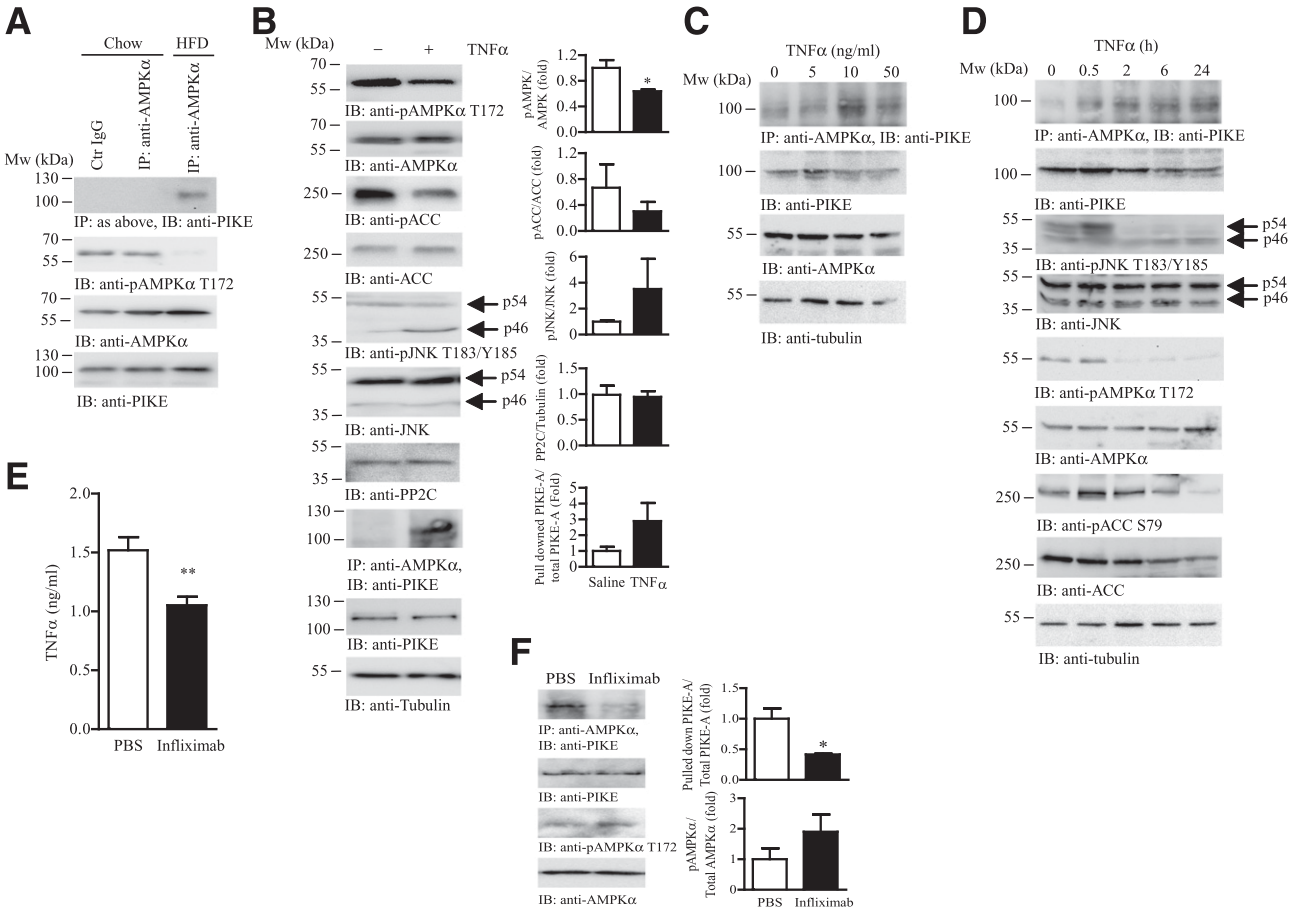

Figure 4—TNF-α promotes PIKE-A and AMPK interaction. *A*: Immunoprecipitation (IP) of AMPK was performed using the hind limb skeletal muscle (mixed fiber type) isolated from chow- or HFD-fed (60% kcal, 12 weeks) female mice. The associated PIKE-A was determined by Western blotting. The amount of phosphorylated AMPKα (pAMPKα), total AMPKα, and PIKE-A in the input were also determined by immunoblotting (IB). Data are representative results from two different mice in each feeding group. *B*: Immunoprecipitation of AMPK was performed using the hind limb skeletal muscle (mixed fiber type) isolated from PBS- or TNF-α–infused (1 μg/kg/day) female mice. The associated PIKE-A was determined by Western blotting. Expression and phosphorylation of AMPK, ACC (pACC), JNK (pJNK), PP2C, PIKE-A, and tubulin in the muscle were also verified. Quantification of the Western blot analysis is also shown in the right panel (*$P < 0.05$, Student *t* test; $n = 3$). *C*: C2C12 myotubes were stimulated with TNF-α of various concentrations for 24 h. AMPK was then immunoprecipitated, and the associated PIKE-A was detected using immunoblotting. Expressions of AMPK, PIKE-A, and tubulin were also determined. *D*: C2C12 myotubes were stimulated with TNF-α (10 ng/mL) for various time intervals. AMPK was then immunoprecipitated and the associated PIKE-A was detected using immunoblotting. Expressions and phosphorylations of AMPK, ACC, and JNK were also determined. Moreover, expression of tubulin and PIKE were verified to ensure equal loading. *E*: Circulating TNF-α in obese mice that have been treated with PBS or anti–TNF-α antibody (infliximab) for 8 days (**$P < 0.01$, Student *t* test; $n = 5$ to 6). *F*: Immunoprecipitation of AMPK was performed using the hind limb skeletal muscle (mixed fiber type) isolated from PBS- or infliximab-administered obese mice. The associated PIKE-A was determined by Western blotting. The amounts of pAMPKα, total AMPKα, and PIKE-A in the input were also determined by immunoblotting. Quantification of the Western blot analysis is also shown in the right panel (*$P < 0.05$, Student *t* test; $n = 3$).

capacity to oxidize FA, which was revealed by a reduction of cellular OCR in response to PA stimulation (Fig. 5*D*). When PIKE-A was overexpressed, a further reduction of TNF-α–suppressed PA oxidation was detected (Fig. 5*D*). In contrast, depletion of PIKE-A abolished the inhibitory effect of TNF-α on AMPK's kinase activity (Fig. 5*B*). Consequently, silencing *PIKE* expression protected the myotubes from TNF-α–impaired lipid oxidation (Fig. 5*D*).

To further substantiate that muscular PIKE-A is critical for TNF-α–induced AMPK inactivation in vivo, we performed TNF-α infusion in MPKO mice. JNK p46 phosphorylation in the muscles of MPKO and *Fl/Fl* mice were comparable after TNF-α infusion for 24 h (Fig. 5*E*), indicating that TNF-α signaling is conserved even in the absence of PIKE-A. However, downregulation of AMPK phosphorylation was only detected in the TNF-α–infused *Fl/Fl* but not MPKO muscle (Fig. 5*E*), which strongly suggest that the presence of PIKE-A is critical for TNF-α to modulate AMPK activity in vivo. TNF-α infusion did not alter PP2C expression in MPKO muscles (Fig. 5*E*), indicating that the preservation of AMPK phosphorylation in TNF-α–infused MPKO mice is independent of PP2C

Downloaded from http://diabetes.diabetesjournals.org/diabetes/article-pdf/66/7/1858/539888/db160270.pdf by guest on 24 April 2024

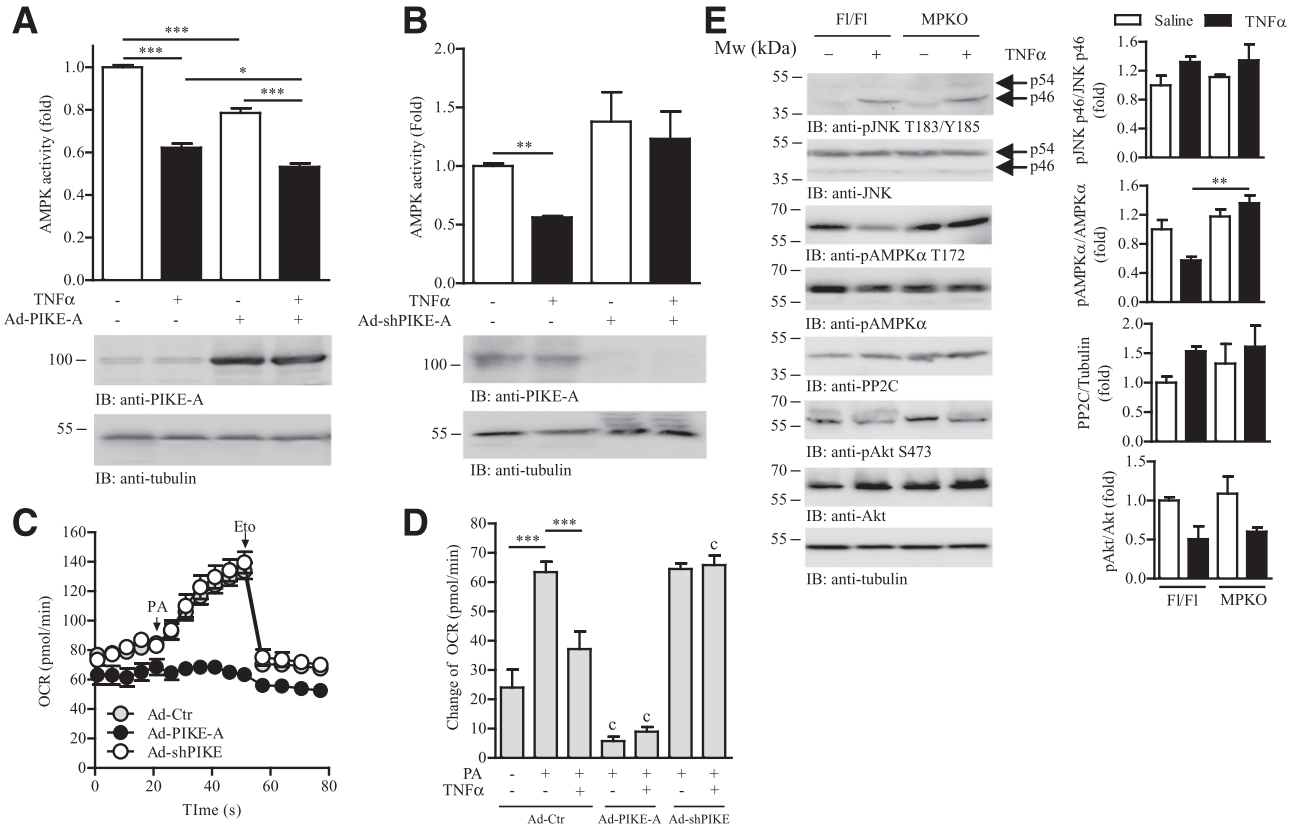

Figure 5—PIKE-A is involved in TNF-α–mediated AMPK inactivation and lipid oxidation. *A*: C2C12 myotubes were infected with control adenovirus (Ad-Ctr) or Ad-PIKE-A. Forty-eight hours after infection, the cells were further stimulated with TNF-α (10 ng/mL) for 24 h. The AMPKα were then immunoprecipitated and used for the in vitro kinase assay. Results were expressed as fold change against the PBS-treated Ad-Ctr–infected cells (top panel; $^{*}P < 0.05$, $^{***}P < 0.001$, one-way ANOVA; $n = 3$). Expression of PIKE-A and tubulin was also determined by immunoblotting (IB; bottom panel). *B*: C2C12 myotubes were infected with Ad-Ctr or Ad-shPIKE. Forty-eight hours after infection, the cells were further stimulated with TNF-α (10 ng/mL) for 24 h. The AMPKα were then immunoprecipitated and used for the in vitro kinase assay. Results were expressed as fold change against the PBS-treated Ad-Ctr–infected cells (top panel; $^{**}P < 0.01$, one-way ANOVA; $n = 3$). Expression of PIKE-A and tubule was determined by Western blot analysis (bottom panel). *C*: A representative profile of OCR in cells infected with Ad-Ctr, Ad-PIKE-A, or Ad-shPIKE for 48 h. The times when PA (1 mmol/L) and etomoxir (Eto; 40 μmol/L) were injected are indicated by arrows ($n = 4$). *D*: Changes of OCR in Ad-Ctr–, Ad-PIKE-A–, or Ad-shPIKE–infected C2C12 myotubes after stimulation by various combinations of TNF-α (10 ng/mL, 24 h) and PA (1 mmol/L) ($^{***}P < 0.01$; $^{c}P < 0.001$ vs. Ad-Ctr–infected cells of the same treatment, Student *t* test; $n = 4$–6). *E*: Immunoblotting analysis of liver and hind limb muscle (mixed fiber type) collected from *Fl/Fl* and MPKO mice after PBS or TNF-α (1 μg/kg/day) infusion for 24 h. Expression and phosphorylations (p) of JNK, AMPK, PP2C, Akt, and tubulin were also verified. Quantification of the Western blot analysis is shown in the right panel ($^{**}P < 0.01$, one-way ANOVA, $n = 3$).

expression. TNF-α suppressed Akt phosphorylation in both Fl/Fl and MPKO muscle (Fig. 5*E*), suggesting PIKE-A is dispensable for TNF-α to modulate insulin/Akt signaling. Similar results were obtained in shPIKE-infected C2C12 myotubes after TNF-α and insulin stimulation (Supplementary Fig. 4). Taken together, our results demonstrate that PIKE-A is an effector of TNF-α to control muscular AMPK activity and cellular lipid oxidation in vitro and in vivo.

PIKE-A Mediates TNF-α–Reduced Mitochondrial Respiration

TNF-α changes cellular bioenergetics via modulating the mitochondrial function in a variety of cell types (37–39). To verify if PIKE-A is also involved in these activities, we investigated the effect of TNF-α on mitochondrial respiration in C2C12 myotubes using an extracellular flux analyzer (Fig. 6*A*). Maximal, but not basal, cellular respiration was significantly decreased after TNF-α stimulation in the control adenovirus–infected cells (Fig. 6*B*). PIKE-A–overexpressed myotubes have a lower basal and maximal respiration than the control cells, and TNF-α stimulation further lowered the maximal respiration (Fig. 6*B*). In contrast, TNF-α–downregulated respiration was abolished when PIKE-A was depleted (Fig. 6*B*). No significant change in cellular glycolysis was detected in PIKE-A–overexpressed or PIKE-A–depleted C2C12 myotubes (Supplementary Fig. 5). The reduced mitochondrial activities were not caused by a change of mitochondrial content, as neither TNF-α stimulation nor PIKE-A expression alters the number of mitochondria in C2C12 myotubes (Fig. 6*C*).

Downloaded from http://diabetes.diabetesjournals.org/diabetes/article-pdf/66/7/1858/539888/db160270.pdf by guest on 24 April 2024

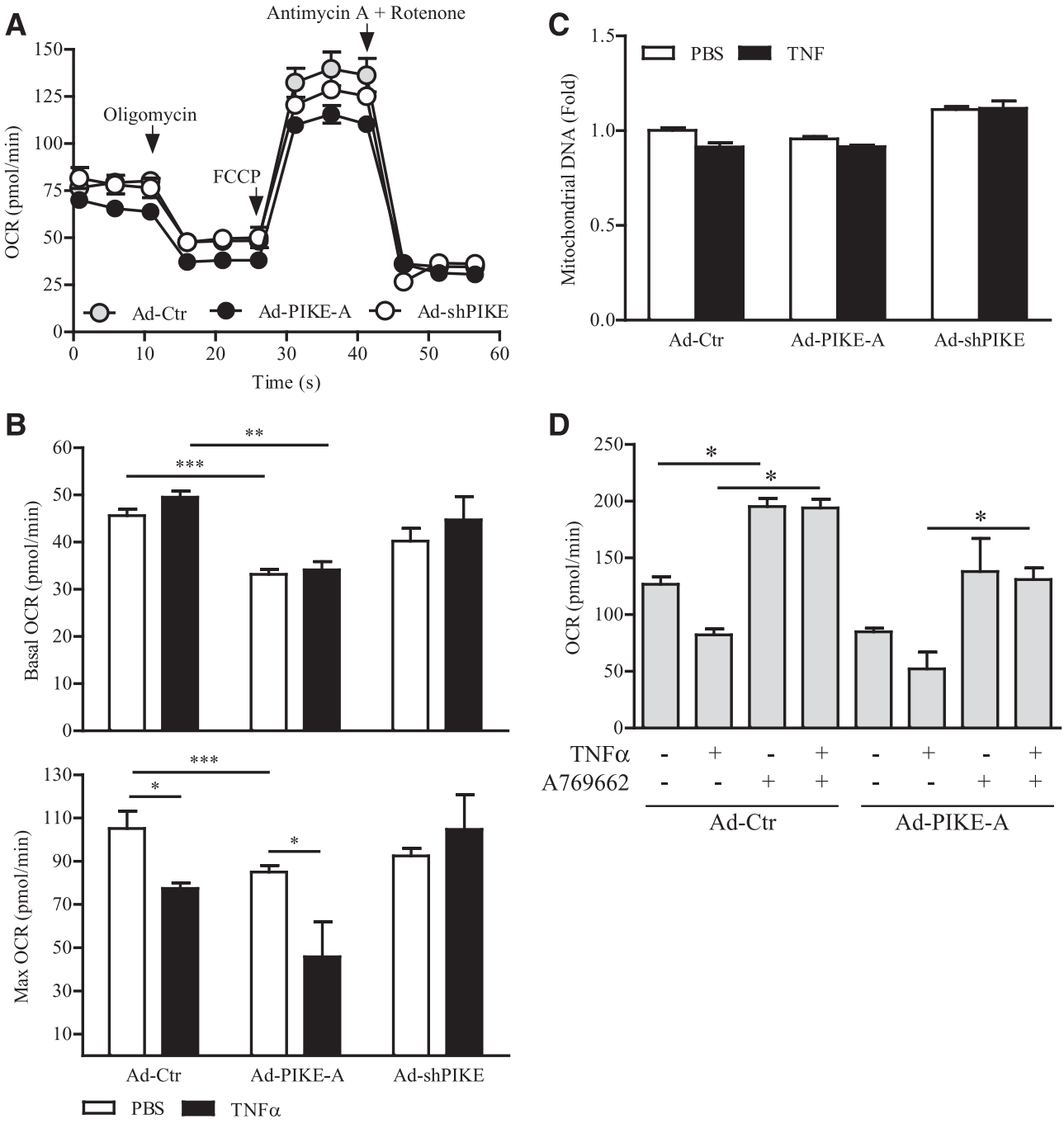

Figure 6—PIKE-A mediates TNF-α–induced mitochondrial respiratory change. *A*: A representative tracing of OCR measured in the control (Ad-Ctr), Ad-PIKE-A, or Ad-shPIKE C2C12 myotubes. The times of oligomycin, carbonyl cyanide-*p*-trifluoromethoxyphenylhydrazone (FCCP), and antimycin A plus rotenone injections are indicated by arrows ($n = 4$). *B*: Basal and maximal mitochondrial respirations of adenovirus-infected C2C12 myotubes (48 h) after 24-h 10 ng/mL TNF stimulation (*$P < 0.05$; **$P < 0.01$; ***$P < 0.001$, one-way ANOVA; $n = 4$–6). *C*: Mitochondrial DNA content in the adenovirus-infected C2C12 myotubes after PBS or TNF-α (10 ng/mL, 24 h) stimulation using real-time PCR methods ($n = 3$). Results were normalized with the amount of actin gene in each sample. *D*: Maximal mitochondrial respiration of adenovirus-infected C2C12 myotubes (48 h) after stimulation by various combinations of TNF-α (10 ng/mL, 24 h) and AMPK activator A769662 (100 μmol/L) (*$P < 0.05$, one-way ANOVA; $n = 3$).

To further investigate if the TNF-α–suppressed cellular respiration is AMPK dependent, we stimulated the C2C12 myotubes with AMPK activator A769662 before TNF-α challenge. As shown in Fig. 6*D*, TNF-α–inhibited cellular respiration was abolished after AMPK activation (Fig. 6*D*). AMPK activation also overwhelmed the respiration defect induced by PIKE-A overexpression in both basal and TNF-α–stimulated cells (Fig. 6*D*), suggesting that AMPK is

Downloaded from http://diabetes.diabetesjournals.org/diabetes/article-pdf/66/7/1858/539888/db160270.pdf by guest on 24 April 2024

the ultimate target of TNF-α and PIKE-A to control cellular respiration.

DISCUSSION

PIKE-A is a downstream effector of various hormones, including prolactin, insulin, and netrin-1 (22,24,40,41). In this report, we further demonstrate that PIKE-A is a new player in TNF-α signaling to control muscular energy metabolism. Our data demonstrate that PIKE-A is needed for TNF-α to suppress AMPK-dependent lipid oxidation and cellular respiration. Ablation of *PIKE* in the skeletal muscle thus prevents the deteriorative effect of TNF-α in lipid metabolisms, especially during obesity development when a large quantity of inflammatory cytokines are produced from the adipose tissue. Consequently, ablation of *PIKE* in the muscle protects the animals from developing excess weight gain, ectopic lipid accumulation, and diabetes development. Combining our recent discoveries that PIKE-A prevents AMPK phosphorylation by liver kinase B1 or Ca^{2+}/calmodulin-dependent protein kinase kinase β (42) and the findings reported in this study, we propose a model that obesity development causes an elevation of circulating TNF-α, which triggers the formation of PIKE-A/AMPK complex in the skeletal muscle. Binding of PIKE-A to AMPK shields the T172 site from being phosphorylated by the upstream kinases. With the additional effect of enhanced dephosphorylation by PP2C (12), the activity of AMPK is impaired in obese muscle, which eventually results in reduced cellular respiration, diminished lipid oxidation, and increased lipid accumulation and insulin resistance.

Previous studies have reported that increasing FA oxidation per se has little effect on adiposity if total energy expenditure remains unchanged (43). Thus, it is logical to question if the augmented AMPK activity in skeletal muscle is the authentic cause of the lean phenotype of MPKO mice, given that the energy expenditure is not altered in these animals. As shown in Fig. 2, it is interesting to note that MPKO mice displayed a reduction of food intake. Because a 10% reduction of calorie intake is sufficient to significantly improve the obesity-induced metabolic deterioration (44), we believe that the diminished food consumption and elevated FA oxidation in skeletal muscle contribute together to reduce the body weight gain in HFD-fed MPKO mice. Nevertheless, how muscular PIKE-A communicates with the brain to control food intake remains to be determined.

By comparing the metabolic phenotypes of $PIKE^{-/-}$, liver-specific *PIKE* knockout (LPKO), and MPKO mice, we have dissected the functional specificity of PIKE-A in different tissues. $PIKE^{-/-}$ and MPKO, but not LPKO, are resistant to diet-induced obesity (22,23), implying that muscular PIKE-A plays the major role in systemic energy metabolism. Hepatic PIKE-A, in contrast, is responsible for IR activation, as we observed no difference in insulin-induced IR activation in the muscle of both $PIKE^{-/-}$ (23) and MPKO mice (Fig. 3). The AMPK regulatory role of PIKE-A is also muscle specific, as we found that LPKO mice have no significant changes in AMPK activity after HFD feeding (23). Because the adipocyte-specific *PIKE* knockout mice are not available, we cannot assess the role of adipose *PIKE* in whole-body metabolism. It is noteworthy that AMPK activities are upregulated in the skeletal muscle of $PIKE^{-/-}$ mice in both chow and HFD feedings (23), but augmented AMPK activity was only observed in HFD-fed MPKO muscle (Fig. 2), suggesting that the negative effect of PIKE-A against muscular AMPK is only significant during energy surplus. This discrepancy also confirms that the increased AMPK activity in $PIKE^{-/-}$ muscle is not a cell-autonomous outcome of *PIKE* ablation. Presumably, the high physical activity of $PIKE^{-/-}$ is the major cause of the elevated AMPK phosphorylation in the muscle. Interestingly, there is a diminution of hepatic ACC expression and phosphorylation in MPKO mice (Fig. 2*H*) that were not detected in the liver of LPKO of $PIKE^{-/-}$ animals (22,23). It remains unknown at current stage why ablation of *PIKE* in the muscle would modify the gene expression in the liver distally, but a change of myokine production is a possible mechanism that requires further study. Nevertheless, our data from MPKO mice studies provide strong evidence that muscular PIKE-A functions as an important component for obesity-induced metabolic changes in the skeletal muscle.

Although TNF-α–suppressed glucose use has been extensively studied, its function in lipid metabolism is far from clear. In particular, the role of TNF-α in FA oxidation seems controversial and species specific. In rat soleus muscle, TNF-α increases the cellular ceramide content without changing the lipid oxidation (45). Similar observation was found in TNF-α–infused human legs muscle (9). In contrast, infusion of TNF-α reduces the FA oxidation rate in conscious dogs (46). Steinberg et al. (12) reported a significant reduction of β-oxidation in TNF-α–stimulated mouse soleus, which could be reverted by administrating anti–TNF-α antibody. Our data from cultured myotubes and in vivo studies support the idea that TNF-α is inhibitory to lipid oxidation by disrupting the AMPK/ACC signaling in mouse (Figs. 4 and 5). We further revealed that TNF-α reduces lipid oxidation in mouse skeletal muscle through promoting PIKE-A/AMPK interaction (Fig. 5).

Interestingly, we found that PIKE-A is important for TNF-α–impaired mitochondrial respiration (Fig. 6). Because AMPK activation is a positive regulator of mitochondrial biogenesis through peroxisome proliferator–activated receptor γ coactivator-1α (47), the diminished AMPK activity in TNF-α–stimulated myotubes possibly could lower the mitochondria concentration, leading to a reduction of cellular capacity for respiration and oxidative phosphorylation. However, we were unable to observe any change of mitochondrial number after TNF-α treatment (Fig. 6), although TNF-α significantly suppresses AMPK activity in myotubes (Fig. 5*A* and *B*). These results imply that the TNF-α–suppressed cellular respiration and FFA oxidation are not caused by a decrease in mitochondria number. Presumably, the reduced AMPK phosphorylation as provoked by PIKE-A interaction may impair the activities of enzymes involved in the electron transport complexes, which results in a decrease

Downloaded from http://diabetes.diabetesjournals.org/diabetes/article-pdf/66/7/1858/539888/db160270.pdf by guest on 24 April 2024

of cellular respiration. In support of this notion, Lantier et al. (48) has reported that decreasing AMPK activity per se is not sufficient to change the mitochondrial content in the muscle but is adequate to reduce the activity of electron transport complexes through an unclear mechanism.

In conclusion, our results indicate that PIKE-A/AMPK interaction is important for TNF-α to regulate lipid oxidation and cellular respiration in skeletal muscle.

Acknowledgments. The authors are thankful to the University of Massachusetts Mouse Metabolic Phenotyping Center for performing the metabolic cage and hyperinsulinemic-euglycemic clamp studies.

Funding. This work is supported by grants from the National Institutes of Health (R01-DK-097092 to C.B.C. and R01-CA-186918 to K.Y.) and the Hong Kong Government Research Grant Council (ECS 27100816 to C.B.C.). Part of this study was performed at the National Mouse Metabolic Phenotyping Center at University of Massachusetts funded by National Institutes of Health grant to Dr. Jason Kim (2U2C-DK093000).

Duality of Interest. No potential conflicts of interest relevant to this article were reported.

Author Contributions. M.C.L.T., O.H.-P., D.B., X.Y., J.W., X.H., Z.L., A.M.Z., and C.B.C. performed the experiments. C.W.L., K.Y., B.K.C.C., and C.B.C. analyzed the data. B.K.C.C., K.Y., and C.B.C. wrote the manuscript. B.K.C.C. and C.B.C. designed the experiments. C.B.C. is the guarantor of this work and, as such, had full access to all the data in the study and takes responsibility for the integrity of the data and the accuracy of the data analysis.

References

1. Aggarwal BB, Gupta SC, Kim JH. Historical perspectives on tumor necrosis factor and its superfamily: 25 years later, a golden journey. Blood 2012;119:651–665

2. Hotamisligil GS, Shargill NS, Spiegelman BM. Adipose expression of tumor necrosis factor-alpha: direct role in obesity-linked insulin resistance. Science 1993; 259:87–91

3. Weisberg SP, McCann D, Desai M, Rosenbaum M, Leibel RL, Ferrante AW Jr. Obesity is associated with macrophage accumulation in adipose tissue. J Clin Invest 2003;112:1796–1808

4. Aguirre V, Uchida T, Yenush L, Davis R, White MF. The c-Jun NH(2)-terminal kinase promotes insulin resistance during association with insulin receptor substrate-1 and phosphorylation of Ser(307). J Biol Chem 2000;275:9047–9054

5. Lang CH, Dobrescu C, Bagby GJ. Tumor necrosis factor impairs insulin action on peripheral glucose disposal and hepatic glucose output. Endocrinology 1992;130:43–52

6. Hotamisligil GS, Murray DL, Choy LN, Spiegelman BM. Tumor necrosis factor alpha inhibits signaling from the insulin receptor. Proc Natl Acad Sci U S A 1994;91: 4854–4858

7. Emanuelli B, Peraldi P, Filloux C, et al. SOCS-3 inhibits insulin signaling and is up-regulated in response to tumor necrosis factor-alpha in the adipose tissue of obese mice. J Biol Chem 2001;276:47944–47949

8. Fernández-Veledo S, Nieto-Vazquez I, Rondinone CM, Lorenzo M. Liver X receptor agonists ameliorate TNFalpha-induced insulin resistance in murine brown adipocytes by downregulating protein tyrosine phosphatase-1B gene expression. Diabetologia 2006;49:3038–3048

9. Plomgaard P, Fischer CP, Ibfelt T, Pedersen BK, van Hall G. Tumor necrosis factor-alpha modulates human in vivo lipolysis. J Clin Endocrinol Metab 2008;93: 543–549

10. Kralisch S, Klein J, Lossner U, et al. Isoproterenol, TNFalpha, and insulin downregulate adipose triglyceride lipase in 3T3-L1 adipocytes. Mol Cell Endocrinol 2005;240:43–49

11. Sumida M, Sekiya K, Okuda H, Tanaka Y, Shiosaka T. Inhibitory effect of tumor necrosis factor on gene expression of hormone sensitive lipase in 3T3-L1 adipocytes. J Biochem 1990;107:1–2

12. Steinberg GR, Michell BJ, van Denderen BJ, et al. Tumor necrosis factor alpha-induced skeletal muscle insulin resistance involves suppression of AMP-kinase signaling. Cell Metab 2006;4:465–474

13. Hurley RL, Anderson KA, Franzone JM, Kemp BE, Means AR, Witters LA. The Ca2+/calmodulin-dependent protein kinase kinases are AMP-activated protein kinase kinases. J Biol Chem 2005;280:29060–29066

14. Woods A, Johnstone SR, Dickerson K, et al. LKB1 is the upstream kinase in the AMP-activated protein kinase cascade. Curr Biol 2003;13:2004–2008

15. Thomson DM, Winder WW. AMP-activated protein kinase control of fat metabolism in skeletal muscle. Acta Physiol (Oxf) 2009;196:147–154

16. Lindholm CR, Ertel RL, Bauwens JD, Schmuck EG, Mulligan JD, Saupe KW. A high-fat diet decreases AMPK activity in multiple tissues in the absence of hyperglycemia or systemic inflammation in rats. J Physiol Biochem 2013;69:165–175

17. Martin TL, Alquier T, Asakura K, Furukawa N, Preitner F, Kahn BB. Diet-induced obesity alters AMP kinase activity in hypothalamus and skeletal muscle. J Biol Chem 2006;281:18933–18941

18. Hardie DG. AMPK: a key regulator of energy balance in the single cell and the whole organism. Int J Obes 2008;32(Suppl. 4):S7–S12

19. Jackson TR, Kearns BG, Theibert AB. Cytohesins and centaurins: mediators of PI 3-kinase-regulated Arf signaling. Trends Biochem Sci 2000;25:489–495

20. Liu X, Hu Y, Hao C, Rempel SA, Ye K. PIKE-A is a proto-oncogene promoting cell growth, transformation and invasion. Oncogene 2007;26:4918–4927

21. Ahn JY, Hu Y, Kroll TG, Allard P, Ye K. PIKE-A is amplified in human cancers and prevents apoptosis by up-regulating Akt. Proc Natl Acad Sci U S A 2004;101: 6993–6998

22. Chan CB, Liu X, He K, et al. The association of phosphoinositide 3-kinase enhancer A with hepatic insulin receptor enhances its kinase activity. EMBO Rep 2011;12:847–854

23. Chan CB, Liu X, Jung DY, et al. Deficiency of phosphoinositide 3-kinase enhancer protects mice from diet-induced obesity and insulin resistance. Diabetes 2010;59:883–893

24. Chan CB, Liu X, Ensslin MA, et al. PIKE-A is required for prolactin-mediated STAT5a activation in mammary gland development. EMBO J 2010;29:956–968

25. Burattini S, Ferri P, Battistelli M, Curci R, Luchetti F, Falcieri E. C2C12 murine myoblasts as a model of skeletal muscle development: morpho-functional characterization. Eur J Histochem 2004;48:223–233

26. Magnoni LJ, Vraskou Y, Palstra AP, Planas JV. AMP-activated protein kinase plays an important evolutionary conserved role in the regulation of glucose metabolism in fish skeletal muscle cells. PLoS One 2012;7:e31219

27. Noda K, Nakajima S, Godo S, et al. Rho-kinase inhibition ameliorates metabolic disorders through activation of AMPK pathway in mice. PLoS One 2014;9: e110446

28. Furda A, Santos JH, Meyer JN, Van Houten B. Quantitative PCR-based measurement of nuclear and mitochondrial DNA damage and repair in mammalian cells. Methods Mol Biol 2014;1105:419–437

29. Jing E, O'Neill BT, Rardin MJ, et al. Sirt3 regulates metabolic flexibility of skeletal muscle through reversible enzymatic deacetylation. Diabetes 2013;62: 3404–3417

30. Wueest S, Mueller R, Blüher M, et al. Fas (CD95) expression in myeloid cells promotes obesity-induced muscle insulin resistance. EMBO Mol Med 2014;6:43–56

31. Chan CB, Liu X, Pradoldej S, et al. Phosphoinositide 3-kinase enhancer regulates neuronal dendritogenesis and survival in neocortex. J Neurosci 2011;31: 8083–8092

32. Winder WW, Hardie DG. Inactivation of acetyl-CoA carboxylase and activation of AMP-activated protein kinase in muscle during exercise. Am J Physiol 1996;270: E299–E304

33. Cool B, Zinker B, Chiou W, et al. Identification and characterization of a small molecule AMPK activator that treats key components of type 2 diabetes and the metabolic syndrome. Cell Metab 2006;3:403–416

34. Zachariah Tom R, Garcia-Roves PM, Sjögren RJ, et al. Effects of AMPK activation on insulin sensitivity and metabolism in leptin-deficient ob/ob mice. Diabetes 2014;63:1560–1571

Downloaded from http://diabetes.diabetesjournals.org/diabetes/article-pdf/66/7/1858/539888/db160270.pdf by guest on 24 April 2024

35. Kim KA, Gu W, Lee IA, Joh EH, Kim DH. High fat diet-induced gut microbiota exacerbates inflammation and obesity in mice via the TLR4 signaling pathway. PLoS One 2012;7:e47713
36. Araújo EP, De Souza CT, Ueno M, et al. Infliximab restores glucose homeostasis in an animal model of diet-induced obesity and diabetes. Endocrinology 2007;148:5991–5997
37. Geng Y, Hansson GK, Holme E. Interferon-gamma and tumor necrosis factor synergize to induce nitric oxide production and inhibit mitochondrial respiration in vascular smooth muscle cells. Circ Res 1992;71:1268–1276
38. Jia L, Kelsey SM, Grahn MF, Jiang XR, Newland AC. Increased activity and sensitivity of mitochondrial respiratory enzymes to tumor necrosis factor alpha-mediated inhibition is associated with increased cytotoxicity in drug-resistant leukemic cell lines. Blood 1996;87:2401–2410
39. Lacerda L, McCarthy J, Mungly SF, et al. TNFα protects cardiac mitochondria independently of its cell surface receptors. Basic Res Cardiol 2010;105:751–762
40. He K, Jang SW, Joshi J, Yoo MH, Ye K. Akt-phosphorylated PIKE-A inhibits UNC5B-induced apoptosis in cancer cell lines in a p53-dependent manner. Mol Biol Cell 2011;22:1943–1954
41. Tse MC, Liu X, Yang S, Ye K, Chan CB. Fyn regulates adipogenesis by promoting PIKE-A/STAT5a interaction. Mol Cell Biol 2013;33:1797–1808
42. Zhang S, Qi Q, Chan CB, et al. Fyn-phosphorylated PIKE-A binds and inhibits AMPK signaling, blocking its tumor suppressive activity. Cell Death Differ 2016;23:52–63
43. Hoehn KL, Turner N, Swarbrick MM, et al. Acute or chronic upregulation of mitochondrial fatty acid oxidation has no net effect on whole-body energy expenditure or adiposity. Cell Metab 2010;11:70–76
44. Wang J, Vanegas SM, Du X, et al. Caloric restriction favorably impacts metabolic and immune/inflammatory profiles in obese mice but curcumin/piperine consumption adds no further benefit. Nutr Metab (Lond) 2013;10:29
45. Bruce CR, Dyck DJ. Cytokine regulation of skeletal muscle fatty acid metabolism: effect of interleukin-6 and tumor necrosis factor-alpha. Am J Physiol Endocrinol Metab 2004;287:E616–E621
46. Sakurai Y, Zhang XU, Wolfe RR. Short-term effects of tumor necrosis factor on energy and substrate metabolism in dogs. J Clin Invest 1993;91:2437–2445
47. Jäger S, Handschin C, St-Pierre J, Spiegelman BM. AMP-activated protein kinase (AMPK) action in skeletal muscle via direct phosphorylation of PGC-1alpha. Proc Natl Acad Sci U S A 2007;104:12017–12022
48. Lantier L, Fentz J, Mounier R, et al. AMPK controls exercise endurance, mitochondrial oxidative capacity, and skeletal muscle integrity. FASEB J 2014;28:3211–3224

Downloaded from http://diabetes.diabetesjournals.org/diabetes/article-pdf/66/7/1858/539888/db160270.pdf by guest on 24 April 2024